Heliyon 10 (2024) e26604

Contents lists available at ScienceDirect

Heliyon

journal homepage: www.cell.com/heliyon

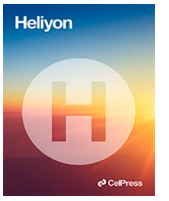

Research article

# Exercise potentially prevents colorectal cancer liver metastases by suppressing tumor epithelial cell stemness *via* *RPS4X downregulation*

Renwen Wan [a,1], Yisheng Chen [a,1], Xinting Feng [a,1], Zhiwen Luo [a,1], Zhen Peng [b], Beijie Qi [c], Haocheng Qin [d], Jinrong Lin [a], Shiyi Chen [a,*], Liangfeng Xu [e,**], Jiayin Tang [f,***], Ting Zhang [g,****]

[a] *Department of Sports Medicine, Huashan Hospital, Fudan University, Shanghai 200040, China*
[b] *Department of Sports Medicine, Shanghai General Hospital, Shanghai Jiao Tong University, Shanghai, China*
[c] *Department of Orthopedics, Shanghai Pudong Hospital, Fudan University Affiliated Pudong Medical Center, Shanghai 201399, China*
[d] *Department of Rehabilitation Medicine, Huashan Hospital, Fudan University, Shanghai 200040, China*
[e] *Department of Gastroenterology, Sheyang County People's Hospital, Yancheng 224300, Jiangsu, China*
[f] *Department of Gastrointestinal Surgery, Renji Hospital, Shanghai 200127, China*
[g] *Department of Integrative Medicine, Huashan Hospital, Fudan University, Shanghai, China*

A R T I C L E I N F O

*Keywords:*
Colorectal cancer
Exercise
Single-cell analysis
Stemness
Epithelial-mesenchymal transition
Apoptosis

A B S T R A C T

*Background:* Colorectal cancer (CRC) is the third most prevalent tumor globally. The liver is the most common site for CRC metastasis, and the involvement of the liver is a common cause of death in patients with late-stage CRC. Consequently, mitigating CRC liver metastasis (CRLM) is key to improving CRC prognosis and increasing survival. Exercise has been shown to be an effective method of improving the prognosis of many tumor types. However, the ability of exercise to inhibit CRLM is yet to be thoroughly investigated.

*Methods:* The GSE157600 and GSE97084 datasets were used for analysis. A pan-cancer dataset which was uniformly normalized was downloaded and analyzed from the UCSC database: TCGA, TARGET, GTEx (PANCAN, n = 19,131, G = 60,499). Several advanced bioinformatics analyses were conducted, including single-cell sequencing analysis, correlation algorithm, and prognostic screen. CRC tumor microarray (TMA) as well as cell/animal experiments are used to further validate the results of the analysis.

*Results:* The greatest variability was found in epithelial cells from the tumor group. *RPS4X* was generally upregulated in all types of CRC, while exercise downregulated *RPS4X* expression. A lowered expression of *RPS4X* may prolong tumor survival and reduce CRC metastasis. RPS4X and

* Corresponding author. Department of Sports Medicine, Huashan Hospital, Fudan University, No. 12 Wulumuqi Zhong Road, Shanghai 200040, China.
** Corresponding author.
*** Corresponding author. Department of gastrointestinal surgery, Renji Hospital, School of Medicine, Shanghai Jiao Tong University, Shanghai 200127, China.
**** Corresponding author.
*E-mail addresses:* cshiyi@163.com (S. Chen), liangfengxu305@163.com (L. Xu), jiayintang@hotmail.com (J. Tang), cczthd18@gmail.com (T. Zhang).
[1] Wan RW, Chen YS, Feng Xinting, and Luo ZW contributed equally to this study.

https://doi.org/10.1016/j.heliyon.2024.e26604
Received 5 February 2024; Accepted 15 February 2024
Available online 24 February 2024

tumor stemness marker-CD44 were highly positively correlated and knockdown of RPS4X expression reduced tumor stemness both in *vitro* and in *vivo*.
*Conclusion: RPS4X* upregulation may enhance CRC stemness and increase the odds of metastasis. Exercise may reduce CRC metastasis through the regulation of *RPS4X*.

## 1. Introduction

Colorectal cancer (CRC) is the third most common cancer and the second leading cause of cancer-related deaths worldwide [1,2]. The 2018 Global Malignancy Statistics Report showed that CRC accounted for 9.2% of malignant deaths, with approximately 1.84 million new CRC cases and 880,000 new deaths reported worldwide [3]. Metastasis is a significant driver of CRC-related deaths, reporting a five-year survival rate of less than 10% when metastases reach a distant site [4]. The liver is the most common metastatic organ of CRC [5], attributable to the blood's circulatory pathway between the liver and the gastrointestinal tract that allows cancer cells to metastasize to the liver parenchyma. Moreover, patients with early-stage CRC have insidious symptoms that are easily missed, while most patients with CRC liver metastasis (CRLM) cannot undergo surgeries leading to poor overall prognosis and survival rate [6], thus, complicating CRC treatment. Therefore, it is key for CRC to be diagnosed early and to suppress the metastasis rate. One approach that scientists are considering is the link between stemness and metastasis.

Stemness is currently defined as the ability of cellular self-renewal and differentiation, although it was previously assumed to be the capacity of healthy stem cells to give rise to all cell types in adult animals [7,8]. Similar to stem cells, some tumor cells, called cancer stem cells (CSCs), can self-renew and expand, and are involved in tumor growth, maintenance, metastasis, and recurrence [9]. The process through which cells lose their epithelial traits and gain mesenchymal ones is known as an epithelial-mesenchymal transition (EMT) [10,11]. During EMT, one of the pathways enhances tumor stem cells' function, cell proliferation, and remote metastasis. Studies have revealed that EMT is a significant factor in the spread of CRC and is closely linked to the aggressive or metastatic characteristics of CRLM. During an EMT-initiated tumor cell metastasis, tumor cells acquire stem cell-like self-renewal properties, forming the metastatic foci [12]. EMT is a fundamental event for tumor cells to develop the capacity to invade and migrate. However, recovery of the epithelial phenotype is still needed for the ability to colonize distant sites. Therefore, the mechanism reflects the importance of epithelial cells in the growth of tumors. Tumor epithelial cells are susceptible to EMT and acquire stem cell-like characteristics of CSCs to metastasize [13,14]. An enhanced tumor stemness mediates treatment tolerance and supports tumor recurrence and distant metastasis [15]. In addition to conventional treatments, one of the most promising methods to remove cancers more effectively is to target CSCs [16]. One of the emerging ways to target CSCs is physical activity.

Evidence shows that physical activity improves human health and is associated with a reduced risk of death, and a lower incidence of cancers [17–19]. Some scholars suggest that adopting exercise after the diagnosis of certain solid tumors, may slow down disease progression and reduce cancer-related mortality [20]. Additionally, although available data suggest that exercise inhibits tumor growth, the underlying mechanisms are yet to be clearly understood. A study has shown that exercise inhibits tumor growth and metastasis by altering the tumor microenvironment (TME) [21–23], partly through the metabolic adaptation of skeletal muscles to exercise [24,25]. During exercise, changes similar to an inflammatory response occur in skeletal muscles, increasing systemic blood circulation, NK cell mobilization, and the level of immune chemokines in tumor patients, thus altering the TME. Changes to TME will increase immune activation and sensitivity towards tumor detection. It has also been shown that exercise affects the stemness of tumor cells [26–28], and reduces their metastasis.

For instance, running upregulates pathways associated with the immune function of mice, which consequently induces a selective mobilization of interleukin (IL)-6-sensitive NK cells and enhances NK cell infiltration to tumor tissues, thereby controlling tumor growth [29]. Long-term exercise is effective in suppressing the viability of cancer cells in patients with prostate cancer [30]; Kurz et al. [31] found that antitumor activity and immune activation could be achieved through exercise due to the activation of IL-15 targets. Collectively, these studies show that exercise activates a network of transcription factors, kinases, and co-regulatory proteins, ultimately causing changes in gene expression and affecting tumor growth, as well as metastasis. Encouraging data from these studies are supporting evidence to further evaluate the molecular effects of exercise in cancers like CRC. In this work, we analyze changes to gene expression in CRLM tumor cells and normal liver cells using single-cell data and explore potential mechanisms that exercise could downregulate tumor stemness in CRC.

## 2. Materials and METHODS

### 2.1. Data acquisition and collation

Datasets were obtained from The Gene Expression Omnibus database. A dataset of mice hepatic immune cells with and without CRC liver metastases was obtained from single-cell RNA sequencing of GSE157600. The gene dataset for campaign upregulation was derived from GSE97084 and includes RNA sequencing of skeletal muscle biopsies from 60 participants from different age and gender groups before and after exercise [32]. This dataset was obtained from a prospective exercise training study that was approved by the Mayo Clinic Institutional Review Board and registered at https://clinicaltrials.gov (#NCT01477164). The study was conducted following the Declaration of Helsinki, and all participants provided informed written consent. The participants were recruited into two distinct age groups: young (18–30 years) or older (65–80 years) with a goal of an equal number of men and women. Participants were

randomly assigned to either the exercise group or the sedentary group. Analysis of variance was performed using the "LIMMA" package in R software as previously described [33]. Both mean expression values and log fold change (logFC) were noted. Differences with an adjusted *P* value of 0.05 or less were regarded as statistically significant [34,35]. GSVA package in R software was used for lollipop mapping, while heat mapping was performed using R's "pheatmap" package. Baseline information sheet data were obtained from level 3 HTSeq-Fragments Per Kilobase Per Million (FPKM) format RNAseq data from the TCGA (https://portal.gdc.cancer.gov/) COADREAD (Colorectal Cancer) project, and FPKM formatted RNAseq data was translated using the log2 function into transcripts per million reads format.

### 2.2. Clustering and annotating subgroups of single cells

Treatment control, clustering, etc. was done for GSE157600 dataset utilizing R software's "Seurat" package [34,36–38]. After normalizing gene expression, "FindVariableFeatures" was used to determine variable genes between samples. The data was first dimensionally reduced using the principal component analysis (PCA) method, followed by further dimensionality reduction using the UMAP and tSNE methods [39,40]. The initial annotation of cell clustering was performed using SingleR [41]. Bulk RNA data using DEseq2 revealed varied gene expression based on the different groups [42]. The cellular activity of scRNA-seq data was analyzed using CytoTRACE, based on a previous study [43].

### 2.3. Prevalent expression profile and immune infiltration analysis of RPS4X in colon cancer

Gene expression matrices of CRC cell lines were obtained from the CCLE dataset (https://portals.broadinstitute.org/ccle/about). The presented analysis was created using the "ggplot2" package (v3.3.3) in R software (v4.0.3) [44]. RNAseq data were extracted from the TCGA (https://portal.gdc.cancer.gov/) COADREAD (colorectal cancer) project, including the filter control or normal data. The GSVA package (v1.34.0) in R software (v3.6.3) was used for statistical analysis and visualization [45,46].

### 2.4. Survival prediction of key genes

Extraction of RNA-seq expression data and clinical information from the TCGA database for colorectal cancer patients Data were extracted from the TCGA database, a public repository containing a large amount of cancer-related data. For our research question, data were extracted for stage M1, i.e. cancer cases with distant metastases. Then, the Kaplan-Meier (KM) method was used to plot the survivorship curves. The log-rank test was used to calculate statistical differences between groups with high and low expression of target mRNA. Finally, the risk ratio (HR) was calculated to estimate the strength and direction of association between target mRNA high and low expression levels and OS.

### 2.5. Immune landscape analysis of RPS4X

Standardized pan-cancer datasets were downloaded from the UCSC (https://xenabrowser.net/) database: TCGA, TARGET, GTEx (PANCAN, $n = 19{,}131$, $G = 60{,}499$). Additionally, the ENSG00000198034 (RPS4X) gene, 60 genes of two types of immune checkpoint pathways (Inhibitory (24), Stimulatory (36)), and expression data of marker genes were extracted from the literature [47] for each sample. Samples were sourced from Primary Solid Tumor, Primary Tumor, Primary Blood-Derived Cancer-Bone Marrow, and Primary Blood-Derived Cancer-Peripheral Blood and then screened. We also filtered all normal samples, and further log2(x+0.001) transformed each expression value. Pearson correlation was then calculated ENSG00000198034 (RPS4X), and the five classes of immune pathway marker genes were denoted [48].

### 2.6. RPS4X and TME score and mutation landscape analysis

Based on a previous report [49], we used the "estimate" package (v1.0.13) in R software (v3.6.3) [50] with the algorithms StromalScore, ImmuneScore, ESTIMATEScore to analyze the correlation between RPS4X (ENSG00000198034) and immune cells as a reflection of the relevance of *RPS4X* to TME assessment. Differences in the frequency of gene mutations in each set of samples were subsequently assessed using Chi-square tests.

Six tumor stemness indices were calculated from mRNA expression and methylation signatures were obtained from previous studies [9] as follows: RNA-based Stemness Scores were derived from the Stemness group. RNAss: RNA expression-based (all set of available genes) which score will drive the main figures in PancanAtlas paper. EREG. EXPss: Epigenetically regulated RNA expression-based (103 genes). DNA methylation-based Stemness Scores were derived from the Stemness group. DNAss: DNA methylation-based (Stem cell signature probes (219 probes), that combine the three signatures listed below). This score will drive the main figures in the PancanAtlas paper. EREG-METHss: Epigenetically regulated DNA methylation-based (87 probes). DMPss: Differentially methylated probes-based (62 probes). ENHss: Enhancer Elements/DNAmethylation-based (82 probes). Furthermore, we extracted the expression data of ENSG00000198034 (RPS4X) gene in each sample and screened the samples from the Primary Blood-Derived Cancer-Peripheral Blood and Primary Tumor. Tumor stemness scores were calculated by mRNA characterization for each tumor identified, based on prior research [9].

### 2.7. Gene set enrichment analysis of RPS4X-related differential genes and related functional pathways

Based on a previous study [42] RNAseq data downloaded from the TCGA (https://portal.gdc.cancer.gov/) COADREAD (colorectal cancer) project, were used and defined as 0%–50% for the low expression group and 50%–100% for the high expression group. The "DESeq2" package (v1.26.0) in the R software (v3.6.3) was used for the analysis of *RPS4X* genes. The "ggplot2" package (v3.3.3) in R software was used to visualize the gene set with the ID: REACTOME_NEUTROPHIL_DEGRANULATION, REACTOME_SIGNALING_BY_INTERLEUKINS. We used the "clusterProfiler" package in R software (v3.6.3) for Gene Set Enrichment Analysis (GSEA) analysis, with previous studies as a reference [51–53]. Data for the analysis were obtained from the c2. cp.v7.2. symbols.gmt (Curated) and c5. all.v7.2. symbols.gmt (Gene ontology) datasets in the MSigDB Collections gene set database. The selected data met the False discovery rate of $<0.25$ and $P < 0.05$ was found to be significantly enriched conditions.

### 2.8. Cell experiments

#### 2.8.1. Cell culture and treatment

SW48 (catalog KG536) cancer cell lines were purchased from KeyGEN. SW48 Cells were cultured at 37 °C with 5% $CO_2$ in RPMI-1640 media supplemented with 10% FBS. Mycoplasma-free cells were used in all experiments. The transfection process was performed according to protocol with 50 nM Small interfering RNAs (siRNA-RPSX4 and siRNA-control) acquired from RiboBio (Guangzhou, China) and transfection agents.

#### 2.8.2. CCK-8 assay

Suspended SW48 cells were seeded into a 96-well plate at a cell density of $3 \times 10^4$ cells/mL (100 μL/well) and incubated at 37 °C in a $CO_2$-regulated environment. Afterward, 10 μL of CCK-8 reagent was added to each well and the plate was incubated for 2 h. The optical density of each well was then measured at 450 nm using a microplate reader.

#### 2.8.3. In vitro migration and invasion assays

In order to assess cell migration and invasion, Transwell chambers (Corning) were employed; with or without Matrigel (Corning) coating depending on the desired assay. SW48 cells ($1 \times 10^5$) in 200 μL of serum-free medium were seeded in the upper chamber, while 600 μL of medium containing 10% FBS was added to the lower chamber. After 24 h, the cells that had migrated/invaded to the lower surface of the membrane were observed and counted.

#### 2.8.4. Cell apoptosis assay

The apoptosis of treated cells was analyzed by Annexin V-PE/7-AAD Kit (Cat. KGA1016, KeyGEN, Nanjing, China) according to the manufacturer's instructions. Analysis was conducted using the FACSCalibur flow cytometer (BD Biosciences, NJ, USA). Apoptotic data were analyzed utilizing FlowJo7.6 software.

### 2.9. Mouse tumor model

Male BALB/c nude mice (~20 g on average, 5 weeks old) were purchased from Shanghai SLAC Laboratory Animal Co.,Ltd. The mice were raised in SPF-grade experimental animal centers and provided with free access to food and water. All experiments were approved by the Institutional Animal Care and Use Committee of Renji Hospital, School of Medicine, Shanghai Jiao Tong University. To establish the xenografts model, SW48 tumor cells were subcutaneously injected into the flanks of these mice. Tumors were monitored and regularly measured with calipers every two to three days. When tumors reached about 100 $mm^3$ in volume, mice were randomized into two different groups ($n = 5$): the siRNA ctrl group and the siRNA RPS4X group. In vivo, siRNAs were synthesized by RiboBio (Guangzhou, China), and delivered to mice through intra-tumor injection at 50 nmol twice a week. On day 21, the mice were anesthetized with a 0.5% sodium pentobarbital solution to remove the tumor, photographed, and weighed.

### 2.10. Immunohistochemistry and semi-quantitative analysis

CRC tumor microarray (TMA) HCol-Muc060CS-01, which was purchased from Outdo BioTech, contained 30 paired tumor and para-tumor samples. The use of the TMA was approved by the Clinical Research Ethics Committee in Outdo Biotech (Shanghai, China). The TMA was submitted for immunohistochemistry (IHC) assay to define the protein expression of RPS4X in tumor and para-tumor tissues. The primary antibody utilized in the study was anti-RPS4X (1:200 dilution, Cat. 14799-1-AP, ProteinTech, Wuhan, China) and anti-CD44 (ready-to-use, Cat. GM7082, GeneTech, Shanghai, China). Antibody staining was visualized with DAB and hematoxylin counterstain. Stained TMA was evaluated by two independent senior pathologists according to the immunoreactivity score standard [54].

## 3. Results

### 3.1. Transcriptome analysis of liver metastatic tumor tissues

Quality control was first performed on mouse liver metastatic cancer tissues from the GSE157600 dataset. PCA, UMAP, and tSNE

models were used for the downscaling analysis of RNA-seq, to help identify the cluster characteristics of these data. The data before and after de-batching were presented, and the results showed some differences in the composition of cells between the normal and tumor groups (Supplementary Fig. 1A). Cells were clustered by marker genes and divided into 24 clusters (Supplementary Figs. 1B and C), and UAMP profiles showed differences in cell types between the normal and tumor groups (Supplementary Fig. 1D).

Subsequently, the distribution of different cell sets in tumor tissues was demonstrated using UMAP and tSNE plots, respectively, for each group, and the cells in the tumor and normal groups were annotated into 10 cell subpopulations, including Macrophagocyte, Neutrophils, B-cells, T-cells, cDCs, pDCs, cNKs, IrNKs, Epithelium, Basophils subpopulations (Fig. 1A). Comparisons between the tumor, and normal groups showed differences in cell types (Supplementary Figs. 1E and F). The proportion of different cell types in normal and tumor groups was indicated by bar graphs to analyze changes in cell composition in the tumor group (Fig. 1B). It was found that the proportion of epithelial cells in the tumor group that developed liver metastases had significantly increased, suggesting that epithelial cells may be associated with certain mechanisms of CRLM.

The expression levels of marker genes for these ten cell subpopulations were analyzed, to determine if the cell classification was accurate. The marker genes defining the cells in a previous study [55], including Lyz2, Csf1r, and 37 other marker genes were referenced. The expression of these marker genes in various cell types was represented using Violin plots (Fig. 1C). Bubble plots were used to present expression characteristics of marker genes between different cell types in the normal and tumor groups (Supplementary Fig. 2A), which also indicated that this cell annotation can be used to distinguish different cell types.

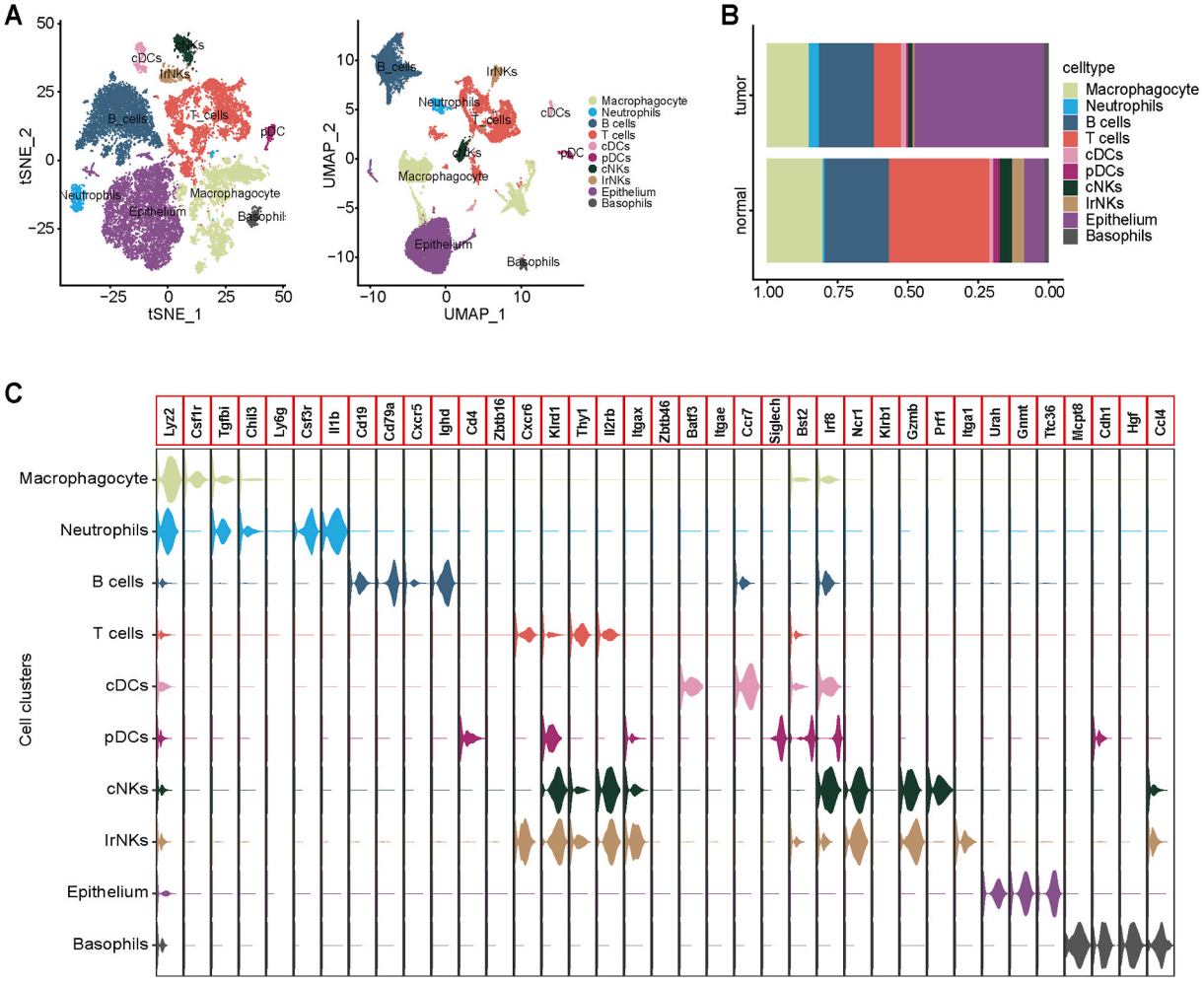


**Fig. 1.** Heterogeneity of the transcriptome and differences in the cellular composition of hepatic immune cells in tumor groups. (A) tSNE and UMAP show the distribution of 10 types of cells in the tumor group, with different colors corresponding to different types of cells. (B) The histogram shows the proportion of different cell types in the tumor and normal groups. (C) Violin diagrams display the expression of marker genes in different cells. Horizontal coordinates represent marker genes and vertical coordinates represent cell types. (For interpretation of the references to color in this figure legend, the reader is referred to the Web version of this article.)

### 3.2. Epithelial cells with high stemness promoted CRC metastasis

To reveal the relationship between the degree of cellular variability and phenotype of these ten cell subpopulations, further analysis was performed. The results of the TRACE macroscopic analysis showed that the epithelial cell phenotype had a large degree of variability (Fig. 2A and B). Subsequently, we analyzed the phenotypic differences of these ten cell subpopulations in the normal and tumor groups. Violin plots showed a large phenotypic difference between the tumor and normal groups for epithelial cells (Fig. 2C). Although the differences between other cell types were also statistically significant, combined with the results in Fig. 1B, where epithelial cells were the most variable cell type in terms of number, we considered the phenotypic changes in epithelial cells to be more meaningful to investigate. This suggests that phenotypic changes in epithelial cells from metastatic liver lesions may be associated with promoting CRC metastasis.

A separate TRACE analysis was also done for epithelial cell characteristics (Fig. 2D), which showed large variability in the tumor group. It was speculated that differences in specific sections of the epithelial cells might be related to the malignant behavior of the tumor. To verify this hypothesis, the epithelial cells were clustered. Additionally, to achieve a better quality of the ARACNe network K nearest neighbor graphs were generated *via* the viperSimilarity distance method followed by integrating the counts of the K of nearest

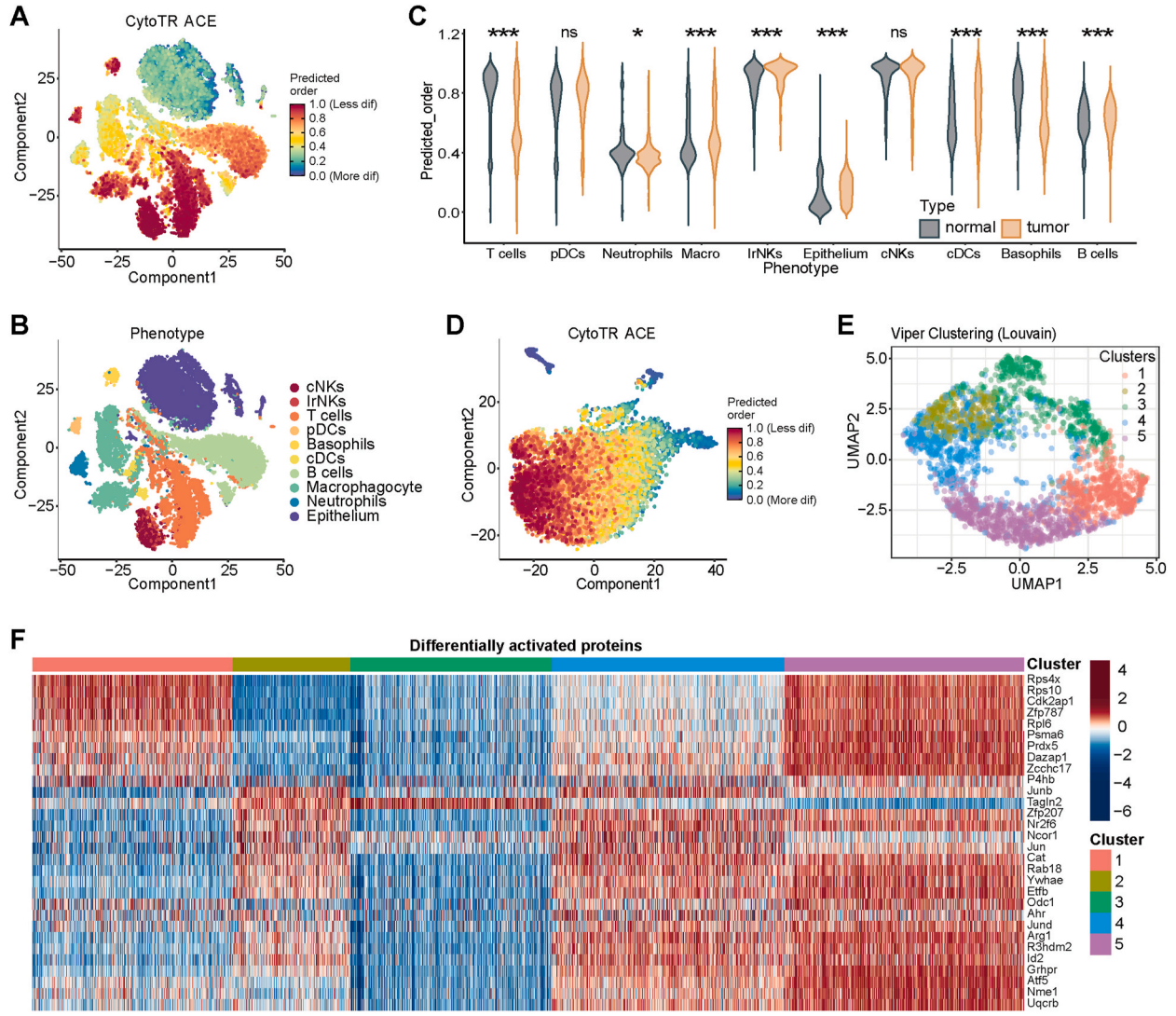


**Fig. 2.** Differentiation characteristics of epithelial cells in colorectal cancer. (A–B) CytoTRACE shows the differences between varied cells in the tumor group and classifies cell clusters by phenotype, with different colors corresponding to different types of cells. (C) Violin plots illustrate phenotypic differences in different cell types in the tumor group *vs.* the normal group, with the horizontal coordinate representing cell type and the vertical coordinate, the prediction coefficient. (D) CytoTRACE depicts the differentiation characteristics of the epithelium. (E) UMAP shows epithelial cells grouped into five clusters according to protein clustering. (F) Heatmap displaying differentially activated proteins between different clusters. (For interpretation of the references to color in this figure legend, the reader is referred to the Web version of this article.)

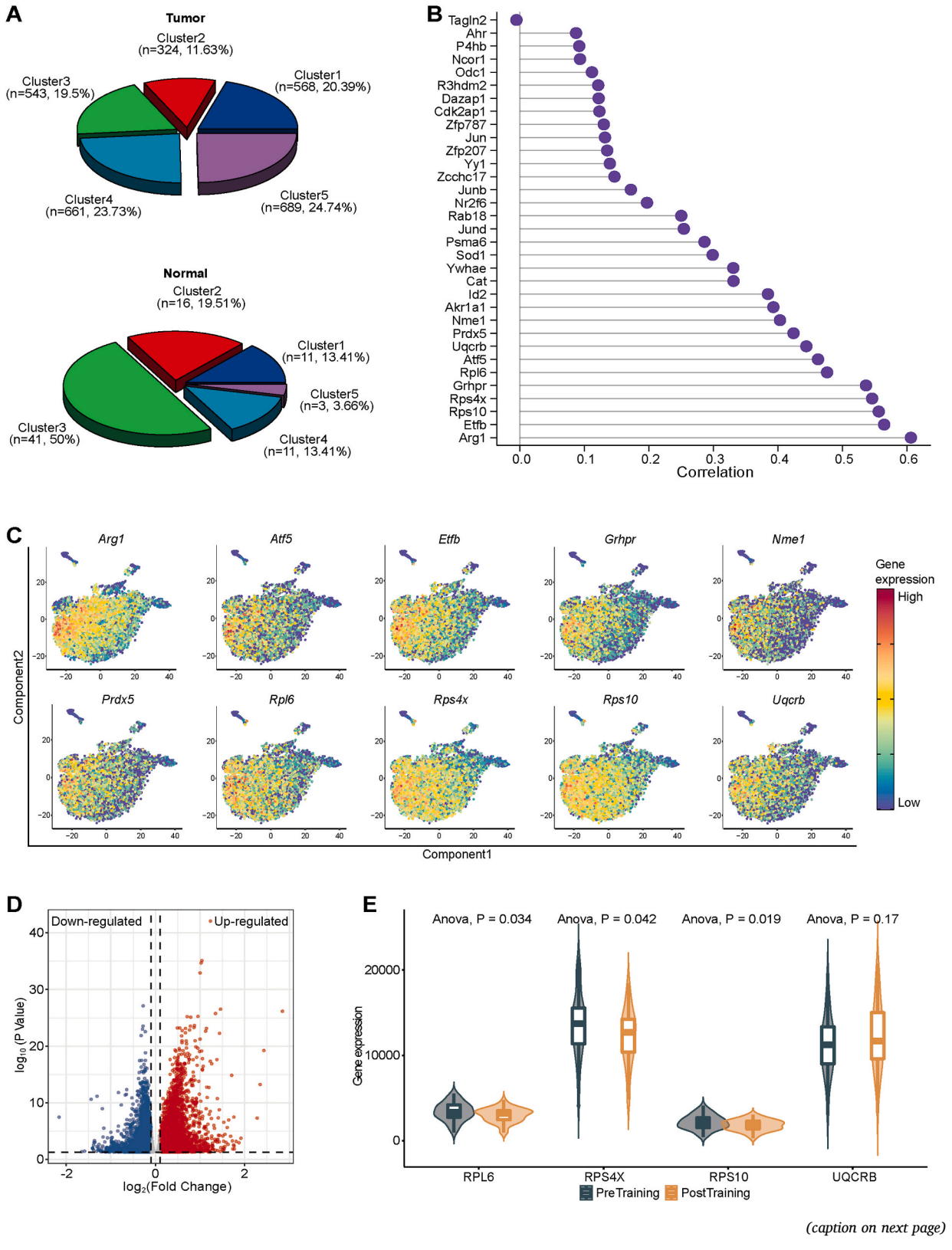


*(caption on next page)*

**Fig. 3.** Cluster analysis of epithelial cells and protein activity of movement regulation. (A) Pie charts show the differences between the clustering compositions of epithelial cells between the normal and tumor groups. (B) Lollipop plot illustrating the degree of association between over 33 protein activities and epithelial cell differentiation. (C) CytoTRACE demonstrates the relationship between the top 10 proteins associated with cell differentiation and epithelial cell activity. (D) Volcano plots displaying changes in the expression of differential genes before and after exercise. (E) Violin plot illustrating the expression changes of *RPL6*, *RPS4X*, *RPS10*, and *UQCRB* genes preTraining and postTraining.

cells. According to a study [55], a silhouette score of 0.25 or above is generally considered robust, as shown by k5 (Supplementary Fig. 2B). Therefore, k5 was chosen, and it was found that epithelial cell protein clusters are divided into 5 species, representing different subgroups of cells (Fig. 2E). Moreover, different epithelial cell activity, particularly differential proteins between clusters (Fig. 2F) were captured by heatmaps. This suggests that a subset of epithelial cells in both tumor and normal tissues were altered and differed in protein expression levels and phenotype. It is hypothesized that this subset of differential epithelial cells plays an important role in the development of tumorigenesis.

### 3.3. Exercise-regulated protein activity

Differences in the clustering of epithelial cell subpopulations between the tumor and normal groups were further analyzed to determine the cluster of epithelial cell subpopulations with greater differences. The pie charts show the differences in the proportion of epithelial cell clustering composition between both groups (Fig. 3A). The smallest proportion of cluster 5 in the normal group and the

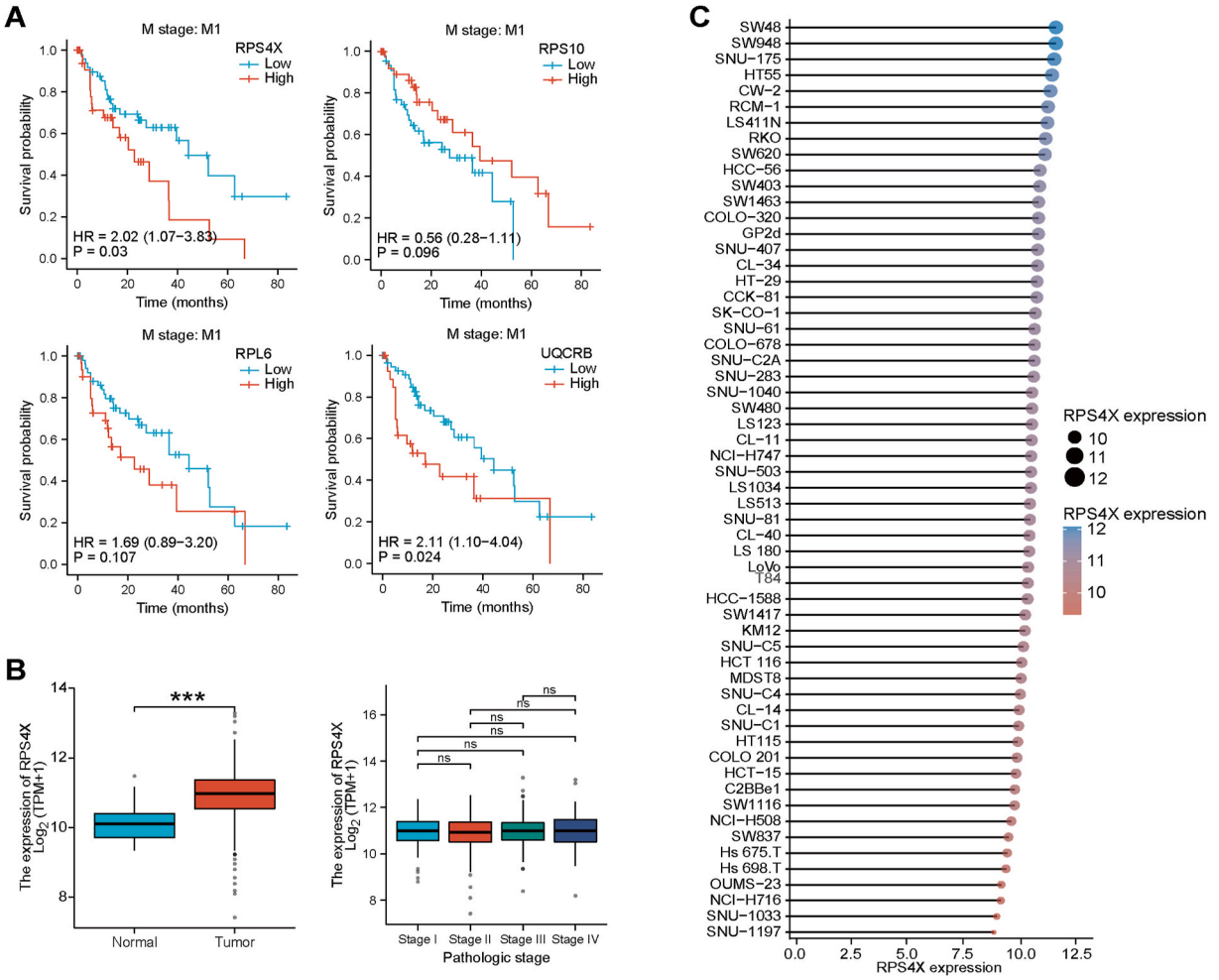


**Fig. 4.** RPS4X levels are associated with prognosis and tumorigenesis. (A) Survival prediction shows the relationship between the expression levels of *RPL6*, *RPS10*, *UQCRB*, and *RPS4X* genes, and tumor survival, with different colors representing the level of gene expression. (B) Box plots show that *RPS4X* is associated with tumorigenesis but not with tumor stage. (C) Expression distribution of *RPS4X* gene in different cell lines. The horizontal coordinates represent the expression level of the gene, while the vertical coordinates are different cell lines. The size of the dots in the graph represents the level of expression, and the different colors also represent the level of expression. (For interpretation of the references to color in this figure legend, the reader is referred to the Web version of this article.)

highest proportion of cluster 5 in the tumor group, suggest a change in the direction of epithelial cell differentiation during tumor progression.

In addition, the relationship between 33 genes and their differentiation was analyzed to identify genes responsible for the altered differentiation of epithelial cells. The lollipop plot revealed the degree of association between these genes and differentiation, the 33 genes used for the analysis were identified based on the heat map in Fig. 2F. These proteins represent different epithelial cell activities, especially the differential proteins between clusters captured in the heat map. The epithelial cell subtypes characterized by these proteins may play an important role in tumorigenesis development. (Fig. 3B). We selected Rps10, Uqcrb, Grhpr, Prdx5, Arg1, Etfb, Nme1, Rpl6, Atf5, and Rps4x, which are the top 10 proteins with the highest level of association with differentiation levels for TRACE analysis. The analysis revealed the effect of different genes on cellular activity (Fig. 3C). Subsequently, a previous study [32] was referred and Volcano plots were used to show upregulated, downregulated, and not significantly different genes after exercise, Data from the GSE97084 database (Fig. 3D). Four genes, particularly, *RPL6*, *RPS4X*, *RPS10*, and *UQCRB*, were identified for their association with epithelial differentiation and their response to exercise. These four genes expressed PreTraining and PostTraining were presented using Violin plots (Fig. 3E).

### 3.4. *RPS4X expression, prognosis, and immune infiltration characteristics in CRC*

The relationship between these four genes and tumor survival, tumor stage, and immune infiltration sensitivity were analyzed for the strongest association with tumors. Survival prediction models showed the relationship between the expression of *RPL6*, *UQCRB*, *RPS10*, and *RPS4X* genes, and tumor prognosis, which found that low expression of *RPS4X* was beneficial for prolonging tumor survival (Fig. 4A). Therefore, *RPS4X* was selected for subsequent analysis. The Box plot demonstrated that the tumor group had higher levels of *RPS4X* expression than the normal group, which suggested its association with tumorigenesis. However, there was no significant correlation between *RPS4X* expression level and tumor stage (Fig. 4B). The *RPS4X* protein expression was assessed in human

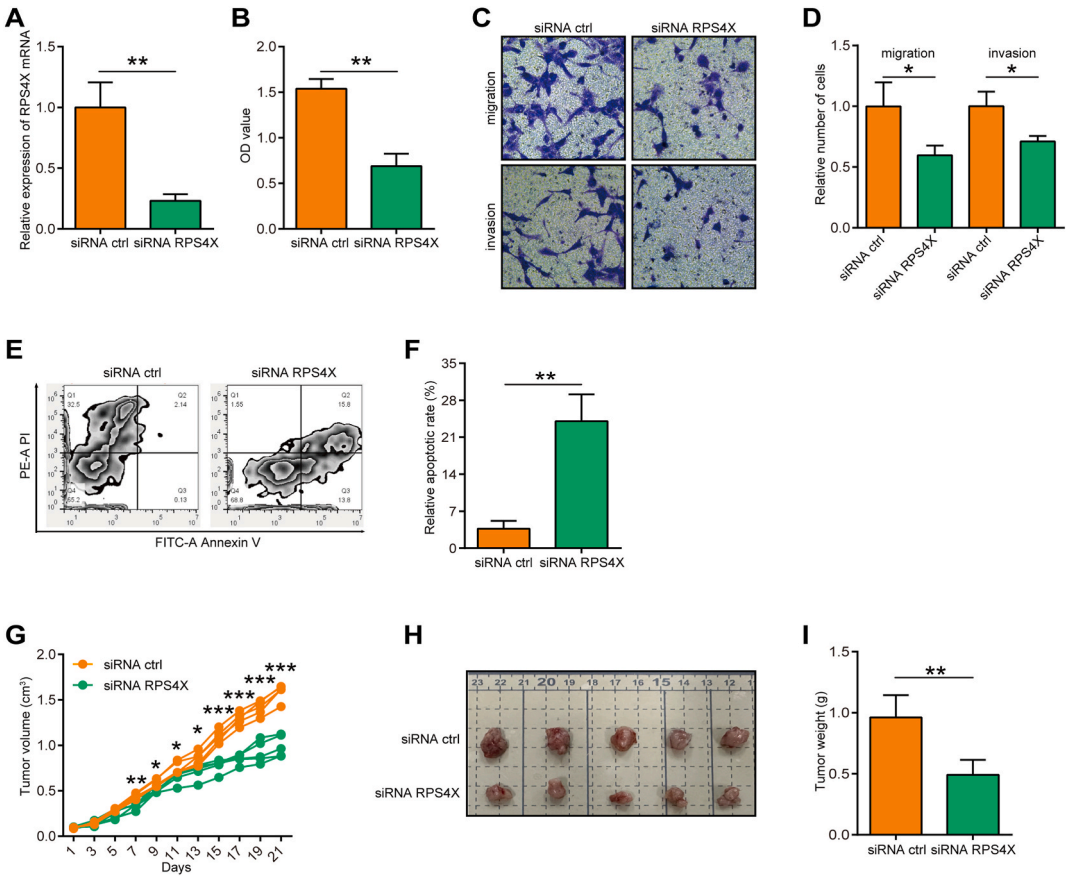


**Fig. 5.** Knockdown of RPS4X expression reduced tumor stemness. (A) The RPS4X gene expression level was assessed by qPCR. GAPDH served as an internal parameter (n = 3). (B) The cell proliferation ability of SW48 was determined using the CCK-8 assay (n = 3). (C–D) Cell migration and invasion ability of SW48 were evaluated (n = 3). Data are presented as mean ± SD. *P < 0.05 (E–F) Cell apoptotic rate of SW48 was evaluated (n = 3). Data are presented as mean ± SD. **P < 0.01. (G) Tumor growth curve and RPS4X down-regulation in tumors from mice (n = 5 per group). Data are presented as mean ± SD. *P < 0.05 **P < 0.01 ***P < 0.001. (H) Representative images showing the tumors harvested from SW48-bearing mice (n = 5 per group). (I)Weight of the harvested tumors from tumor-bearing mice (n = 5 per group). Data are presented as mean ± SD. **P < 0.01.

specimens, and it was significantly upregulated in tumor tissue compared with corresponding para-tumor tissue (Supplementary Figs. 3A–B). To confirm the unique expression of RPS4X in colon cancer, its expression was investigated in various CRC cell lines. The findings revealed that most CRC cell lines expressed RPS4X at high levels (Fig. 4C), indicating that upregulation of this gene is common in CRC.

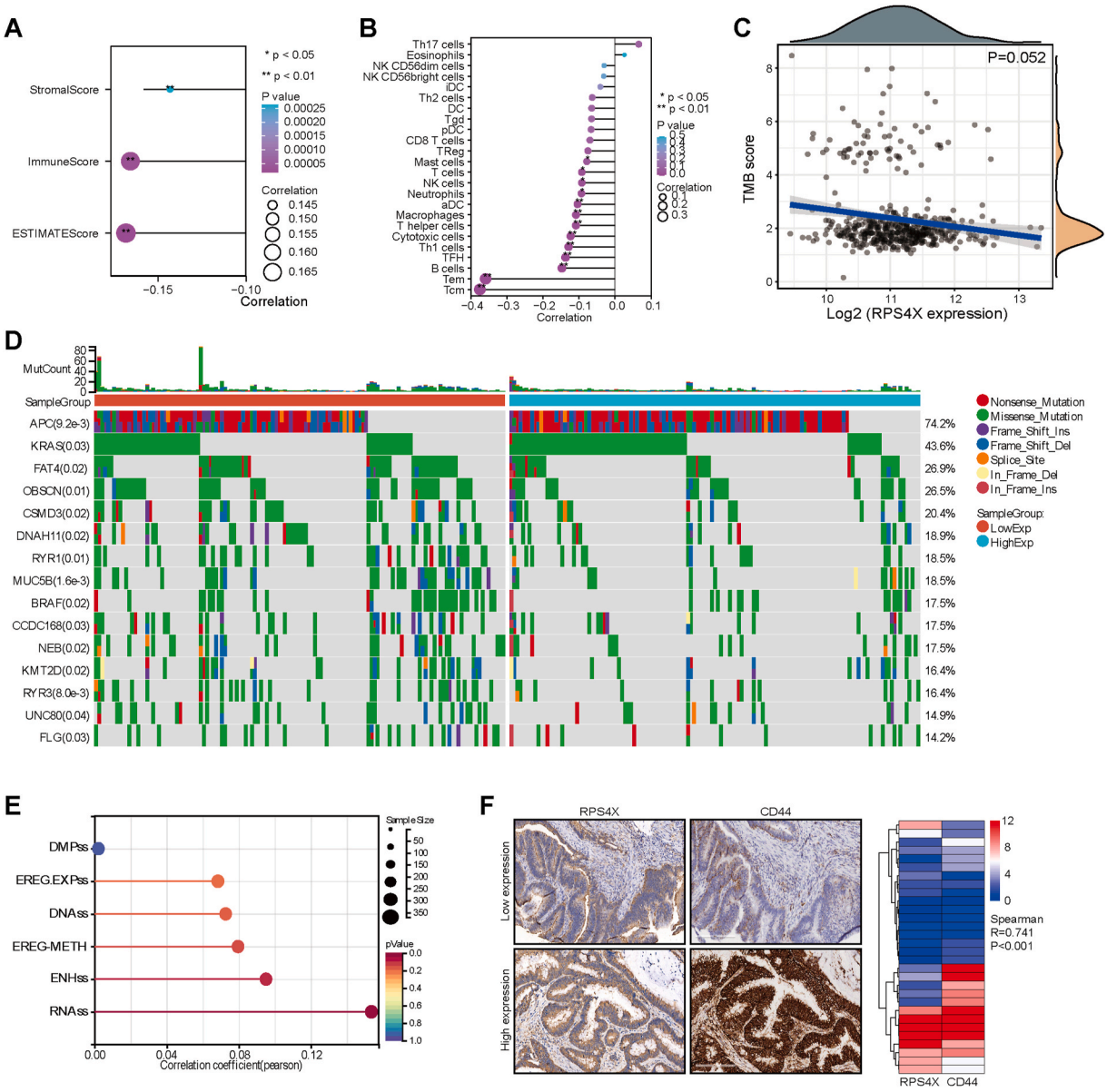


**Fig. 6.** RPS4X and cancer stemness and mutational landscape analysis. (A) The lollipop plot shows a negative correlation between *RPS4X* and the tumor microenvironment score (StromalScore, ImmuneScore, and ESTIMATEScore). The circle size represents the degree of association, and the color represents the p-value size. (B) The lollipop plot reveals that *RPS4X* is negatively correlated with immune infiltration, where the horizontal coordinate represents the correlation coefficient, the vertical coordinate represents the cell type, and the circle size represents the degree of association. (C) *RPS4X* expression level was negatively correlated with tumor mutational burden (TMB) score, horizontal coordinates represent *RPS4X* expression level and vertical coordinates represent TMB score. (D) Heatmap showing the correlation of high and low *RPS4X* expression with the oncogene mutation picture landscape. The number after the abbreviation is the P value of the chi-square test. (E) Lollipop plot displaying the correlation coefficients between *RPS4X* and six tumor stemness indices (DMPss, EREG. EXPss, DNAss, EREG-METH, ENHss, and RNAss). (F) The representative figures in the CRC tumor microarray for CD44 and RPS4X were presented. The correlation of the two proteins was shown in the right heatmap using the Spearman algorithm. (For interpretation of the references to color in this figure legend, the reader is referred to the Web version of this article.)

### 3.5. Knockdown of RPS4X expression reduced tumor stemness both in vitro and in vivo

Next, cell experiments were performed on the SW48 CRC cell line to test the potential role of RPS4X in colon cancer. siRNA RPS4X significantly downregulated the RPS4X mRNA level (Fig. 5A). After the knockdown of RPS4X, the cell proliferation ability (Fig. 5B), cell migration, and invasion ability (Fig. 5C and D) of cancer cells were significantly weakened, and the cell apoptotic rate was notably enhanced (Fig. 5E and F). In addition, inhibition of RPS4X also suppressed tumor growth in vivo (Fig. 5G–I), supporting the significant oncogenic role of RPS4X in colon cancer. In summary, those data indicated that *RPS4X* was speculated as a gene commonly expressed in most CRCs, and its expression level was negatively correlated with tumor prognosis. In addition, inhibition of its expression may reduce the stemness of cancer cells and contribute to cancer treatment.

### 3.6. RPS4X and the immune landscape

The objective of the pan-cancer analysis was to define the immunological function of *RPS4X*, which is critically beneficial in the identification of selected cancer types [56–58]. The expression data of *RPS4X*, and 150 marker genes in five classes of immune pathways (chemokine (41), receptor (18), MHC (21), immunoinhibitor (24), and immunostimulator (46)) were explored in individual samples. The heatmap revealed that *RPS4X* positively correlated with most immunomodulators in the vast majority of cancers (Supplementary Fig. 4A). *RPS4X* with 60 immune checkpoints (24 Inhibitory and 36 Stimulatory) were analyzed and showed that *RPS4X* has the potential as a combinatory agent with immune targeting drugs to enhance the efficacy of immunotherapy (Supplementary Fig. 4B), suggesting that *RPS4X* is expected to be a new target for future tumor therapy.

### 3.7. RPS4X and the tumor stemness/mutation landscape

To investigate the effect of *RPS4X* expression on tumor mutation and tumor stemness, the potential role of *RPS4X* in tumor prognosis and immune drug therapy was analyzed. Firstly, three scoring metrics, StromalScore, ImmuneScore, and ESTIMATEScore, were selected as a measure of TME [59]. The Lollipop plot showed that *RPS4X* had a negative correlation with the TME score (Fig. 6A). Subsequently, the immune infiltration characteristics of *RPS4X* were analyzed, and the Lollipop plot showed a negative correlation between *RPS4X* and immune infiltration (Fig. 6B). Additionally, we discovered a negative connection between the tumor mutation (TMB) score and the degree of *RPS4X* expression (Fig. 6C). Subsequently, we assessed the difference in mutation frequency in each group of samples using the Chi-square test. The landscape map demonstrated an association between tumor mutation and *RPS4X* expression level (Fig. 6D). In our previous study [9], we obtained six tumor stemness indices calculated by mRNA expression and methylation signature, namely RNAss, EREG. EXPss, DNAss, EREG-METHss, DMPss, and ENHss. The results showed that all tumor

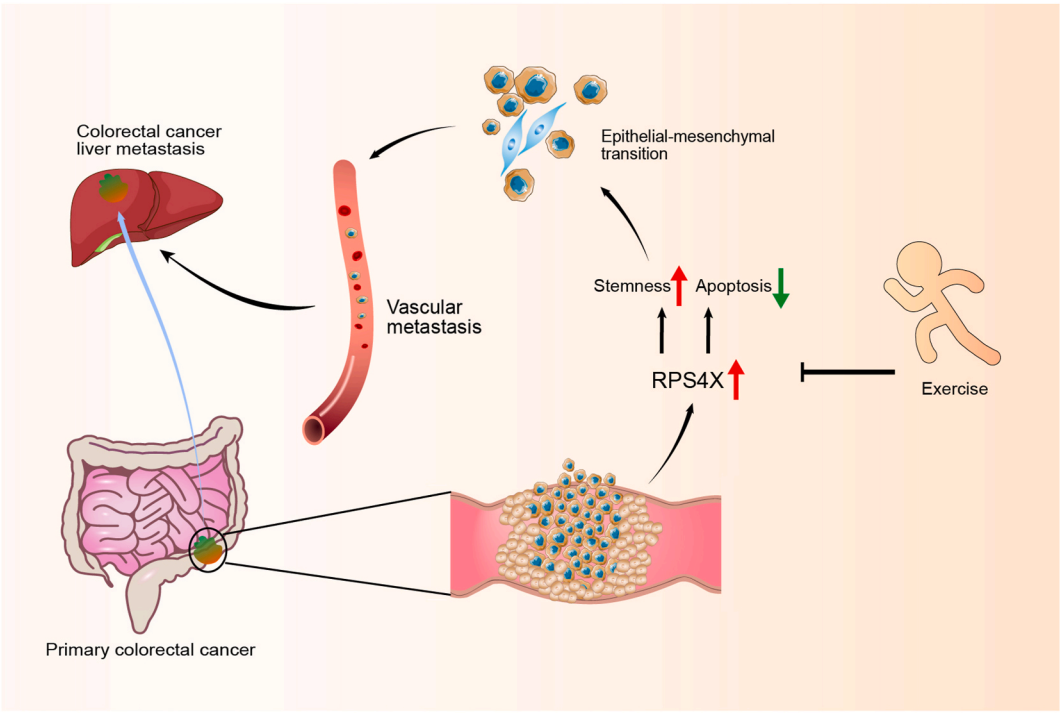


**Fig. 7.** Schematic depiction of this work. Exercise can downregulate RPS4X affecting cancer stemness and might be a potential therapeutic strategy to reduce CRLM.

stemness indices except DMPss were significantly correlated with *RPS4X* expression (Fig. 6E). The results of human specimens from TMA show that RPS4X expression level was significantly correlated with CD44 expression level ($p < 0.001$, $R^2 = 0.741$), which indicated the *RPS4X* was a potential marker for tumor stemness (Fig. 6F, Supplementary Fig. 5).

### 3.8. Results of RPS4X-related functional pathway analysis

To determine the mechanistic pathway of the physiological functions of *RPS4X*, the relationship between *RPS4X* and RNA modifier genes was explored. The correlation between *RPS4X* and related modifier genes of different modifications (m1A, m5C, and m6A) in different tumor samples was also analyzed. The heat map shows a significant relationship between *RPS4X* and immune regulation (Supplementary Fig. 6A), which may suggest that *RPS4X* exerts physiological functions by regulating the expression of RNA modifier genes. Subsequently, an enrichment analysis was performed for potential pathways of *RPS4X*. GSEA pathway analysis revealed that *RPS4X* most likely exerts regulatory effects through the regulatory RNA and RIBONUCLEOPROT pathways (Supplementary Fig. 6B).

## 4. Discussion

In this work, RPS4X expression was found to have a possible strong correlation with the cancer stemness, metastasis, and prognosis of CRC. We found that inhibition of RPS4X expression increased apoptosis in tumor cells. Exercise might be able to downregulate *RPS4X* expression to prevent the progression of CRC. To our knowledge, this is the first evidence to demonstrate that exercise prevents liver metastasis of CRC by reducing tumor epithelial stemness, and a possible potential regulatory molecule-*RPS4X* was revealed (Fig. 7).

Mechanisms in general, according to existing research, have been found that SLFN1 and GTF2E2 can promote tumor growth by activating RPS4X as a downstream effector molecule and through the mTOR pathway. Inhibition of RPS4X can promote tumor cell apoptosis in vitro and inhibit tumor growth in vivo [60,61]. During our research, this was also confirmed, as flow cytometric results showed that inhibition of RPS4X expression contributed to apoptosis and the in *vivo* results suppression of RPS4X indeed reduced the colon tumor growth.

Tumor progression and metastasis have been shown to depend on the TME [62–64], rendering tumors resistant to drugs, and affecting tumor treatment response and clinical outcomes. The targeted remodeling of TME is now considered a new strategy for the treatment of tumors [63,65,66]. The link between RPS4X and TMB was explored and found that RPS4X was negatively correlated with TME scores. We suggest that RPS4X may act as a promotor of tumor growth and metastasis by affecting the TME, with the exact mechanism of action yet to be confirmed.

Another index affecting tumor growth and metastasis is cancer stemness [67,68]. In the current study, a significant correlation between cancer stemness index and *RPS4X* expression was found. As a result, *RPS4X* is considered to be a key factor in regulating cancer stemness, while the TMB is linked to *RPS4X* expression. A GSEA analysis of RPS4X-related functional pathways revealed that the RNA and riboprobe pathways might be the most likely regulatory pathways for *RPS4X* to inhibit tumor epithelial cell stemness. TMA and cell experiments suggested that *RPS4X* was positively correlated with stemness marker-CD44 and knockdown of RPS4X expression reduced tumor stemness.

CSCs behave similarly to stem cells and are referred to as multipotent cancer cells. CSCs are found in various solid tumors, such as colon cancer, breast cancer, and liver cancer [69]. They can generate xenogeneic cancer cells as well as have a self-renewal ability. CSCs are also known as “cancer stemness", *i.e.*, the ability to promote the growth and metastasis of primary tumors [70,71]. Therefore, it is widely believed that CSCs are important for the treatment of tumors and the prevention of their recurrence. For example, Song et al. [72] found that the Oct4 gene was an important target for CSCs and that the stemness of germ cell tumors could be reduced by knocking down Oct4 expression, thus inhibiting tumor growth. Lu et al. [73] further found that miR-26 overexpression could reduce the stemness of osteosarcoma cells by inhibiting the Jagged1/Notch pathway.

Epithelial-mesenchymal transition (EMT) is a process by which epithelial cells lose their polarity and cell-cell adhesion properties, thereby acquiring a mesenchymal phenotype and enhancing their ability to migrate and invade. EMT plays a key role in embryonic development, wound healing, and tumor progression. During cancer metastasis, EMT allows tumor cells to detach from the primary site, invade the blood circulation through the basement membrane, and establish distant metastases. Multiple signaling pathways work together to induce EMT, including TGF-β, Wnt, Notch, EGF, and HGF signaling [74,75]. The EMT serves as an initial step for tumor cells to acquire stemness and is directly related to stemness gain *via* tumor cells. EMT can break the cytoskeleton among tumor cells to facilitate tumor metastasis [76,77]. In our study, we found an increased stemness of tumor epithelial cells in CRLM metastases, and *RPS4X* expression was strongly correlated with the tumor stemness scores. Therefore, although no evidence explains the relationship between *RPS4X* and EMT, it is speculated that an elevated RPS4X increases cancer stemness through EMT, thereby promoting CRC metastasis.

In 1990, researchers isolated the *RPS4X* gene from the human sex chromosomes, which was thought to encode a heterodimer of ribosomal protein S4, and that RPS4X was widely transcribed in human tissues [78]. Now the level of *RPS4X* expression is thought to be a separate factor of prognostic analyses. A low expression of *RPS4X* may be associated with a poor prognosis in plasmacytoid ovarian epithelial carcinoma [79]. Paquet et al. [80] also suggested that a low expression of RPS4X might be associated with a poor prognosis of uroepithelial carcinoma. Interestingly, Kuang et al.’s analysis of RPS4X and the post-surgical prognosis of intrahepatic cholangiocarcinoma showed that a low expression of RPS4X was beneficial for post-surgical survival of patients with intrahepatic cholangiocarcinoma [81]. In our study, we found that the low expression of RPS4X prolonged tumor survival and inhibited cancer stemness.

Exercise has been shown to have a wide range of health benefits. According to a study on Alzheimer's disease, exercise improves the prognosis of patients [38]. Signaling networks within tumors are highly plastic and influenced by multiple extrinsic factors [82], while exercise produces a range of extrinsic factors, including improved blood flow, pH regulation, thermogenesis, and sympathetic activation. This also implies that exercise has a significant potential to modulate cancer progression and biological functions. Historically, patients with cancers were initially advised to rest and avoid strenuous activity after diagnosis, but new studies that challenge this traditional dogma have emerged, and researchers are more willing to believe that exercise can be antitumor [18,83]. An epidemiological study has shown that exercise lowers the risk of developing at least 13 different types of cancers [84].

This may be because, in animal experiments, most exercise intervention studies on rodents have shown that exercise training inhibits tumorigenesis, progression, and metastasis [85]. For example, aerobic exercise may reduce the growth of pancreatic ductal adenocarcinoma by modulating systemic immunity through immune activation and the collection of tumor-infiltrating IL15Rα+ CD8 cells [31]. Exercise has been revealed to have an immunostimulatory effect, which is not associated with major adverse events in tumors and is safe for patients with cancers [86–88]. Furthermore, exercise helps to reduce the side effects associated with cancer treatment and improves the quality of life of patients [89]. Other gene-based studies have also highlighted the positive influence of exercising. A classical signaling pathway associated with tumor formation that inhibits cell growth, the Hippo pathway, was found to be downregulated by exercise [90], suggesting that exercise can reduce tumor formation by affecting the expression of certain proteins to achieve a regulatory effect on tumors. In our study, we found that exercise downregulated the expression of a series of genes, among which the downregulation of RPS4X was closely associated with tumor growth and metastasis. This suggests that one of the potential mechanisms of exercise affecting cancer was achieved through the downregulation of RPS4X. Our in *vitro* and in *vivo* experiments proved this viewpoint that inhibition of RPS4X significantly suppressed tumor growth and promoted cancer cell apoptosis.

Clinical Implications of Exercise in CRC Management: Our study underscores the potential role of exercise as a non-pharmacological intervention in CRC management. Given the observed downregulation of RPS4X and its association with reduced metastasis, we discuss how incorporating exercise regimens into standard CRC care could offer a complementary approach to traditional therapies; We elaborate on how the interplay between exercise and RPS4X expression could pave the way for personalized medicine in CRC treatment. By identifying patients who are likely to respond positively to exercise-induced RPS4X downregulation, clinicians could tailor treatment plans more effectively.

The current study had a few limitations. First, we recognize that our use of cell lines and animal models, while informative, may not fully replicate the complex nature of human colorectal cancer. This includes potential disparities in tumor microenvironment and genetic variability. Second, single-cell sequencing of the metastatic tumors was not performed after exercise, and the effect of exercise on metastatic foci could not be analyzed visually. Third, the GSE157600 dataset was obtained through mouse experiments, while the GSE97084 dataset was obtained through human experiments, and this may have an impact on the analysis results. Further experimental validation and clinical studies are needed on the specific mechanism of exercise against CRLM. In addition, this study lacked comparative studies of RPS4X and other stemness indicators, and follow-up studies could be conducted.

## 5. Conclusion

The results revealed that *RPS4X*, which was downregulated after exercise, might be a key gene affecting cancer stemness. Exercise might be a potential therapeutic strategy to reduce CRLM.

## Ethics approval and consent to participate

The use of the TMA was approved by the Clinical Research Ethics Committee in Outdo Biotech (Shanghai, China, approval no. HCol-Muc060CS-01). All participants provided informed consent before participating in the present study and all methods were performed in accordance with Declaration of Helsinki. In this study, animal experiments were performed according to the National Institutes of Health Guide for the Care and Use of Laboratory Animals. In addition, all the experimental protocols were approved by the Animal Care and Use Committee of Renji Hospital, School of Medicine, Shanghai Jiao Tong University (approval no. RJ-2022-0350).

## Funding

This study was supported by the National Natural Science Foundation of China, No. 82102634, and the Healthy Shanghai Project, No. JKSHZX-2022-02.

## Availability of data and materials

The datasets used or analyzed during the present study are available from the corresponding author upon reasonable request.

## Consent for publication

Not applicable.

## CRediT authorship contribution statement

**Renwen Wan:** Writing – review & editing, Writing – original draft, Visualization, Validation, Supervision, Software, Resources, Project administration, Methodology, Investigation, Funding acquisition, Formal analysis, Data curation, Conceptualization. **Yisheng Chen:** Formal analysis, Data curation, Conceptualization. **Xinting Feng:** Project administration, Methodology, Investigation, Formal analysis, Data curation, Conceptualization. **Zhiwen Luo:** Writing – review & editing, Writing – original draft, Visualization, Validation, Supervision, Software, Resources, Project administration, Methodology, Investigation, Formal analysis, Data curation, Conceptualization. **Zhen Peng:** Formal analysis, Data curation, Conceptualization. **Beijie Qi:** Formal analysis, Data curation, Conceptualization. **Haocheng Qin:** Formal analysis, Data curation, Conceptualization. **Jinrong Lin:** Formal analysis, Data curation, Conceptualization. **Shiyi Chen:** Funding acquisition, Formal analysis, Data curation, Conceptualization. **Liangfeng Xu:** Funding acquisition, Formal analysis, Data curation, Conceptualization. **Jiayin Tang:** Funding acquisition, Formal analysis, Data curation, Conceptualization. **Ting Zhang:** Writing – review & editing, Writing – original draft, Visualization, Validation, Supervision, Software, Resources, Project administration, Methodology, Investigation, Funding acquisition, Formal analysis, Data curation, Conceptualization.

## Declaration of competing interest

The authors declare that they have no known competing financial interests or personal relationships that could have appeared to influence the work reported in this paper.

## Acknowledgments

We thank the Shanghai Institute of Nutrition and Health for providing an experimental platform.

## Appendix A. Supplementary data

Supplementary data to this article can be found online at https://doi.org/10.1016/j.heliyon.2024.e26604.

## References

[1] N. Keum, E. Giovannucci, Global burden of colorectal cancer: emerging trends, risk factors and prevention strategies, Nat. Rev. Gastroenterol. Hepatol. 16 (12) (2019) 713–732.
[2] P. Li, Y. Zhang, Y. Xu, H. Cao, L. Li, Characteristics of CD8+ and CD4+ tissue-resident memory lymphocytes in the gastrointestinal tract, Adv. Gut Microbiome Res. 2022 (2022) 1–12.
[3] F. Bray, J. Ferlay, I. Soerjomataram, R.L. Siegel, L.A. Torre, A. Jemal, Global cancer statistics 2018: GLOBOCAN estimates of incidence and mortality worldwide for 36 cancers in 185 countries, CA A Cancer J. Clin. 68 (6) (2018) 394–424.
[4] R.L. Siegel, K.D. Miller, A. Jemal, Cancer statistics, 2016, CA A Cancer J. Clin. 66 (1) (2016) 7–30.
[5] S.R. Horn, K.C. Stoltzfus, E.J. Lehrer, L.A. Dawson, L. Tchelebi, N.J. Gusani, N.K. Sharma, H. Chen, D.M. Trifiletti, N.G. Zaorsky, Epidemiology of liver metastases, Cancer Epidemiol. 67 (2020) 101760.
[6] D.C. Osei-Bordom, S. Kamarajah, N. Christou, Colorectal cancer, liver metastases and biotherapies, Biomedicines 9 (8) (2021).
[7] W. Zakrzewski, M. Dobrzynski, M. Szymonowicz, Z. Rybak, Stem cells: past, present, and future, Stem Cell Res. Ther. 10 (1) (2019) 68.
[8] H. Zheng, H. Liu, H. Li, W. Dou, X. Wang, Weighted gene Co-expression network analysis identifies a cancer-associated fibroblast signature for predicting prognosis and therapeutic responses in gastric cancer, Front. Mol. Biosci. 8 (2021) 744677.
[9] T.M. Malta, A. Sokolov, A.J. Gentles, T. Burzykowski, L. Poisson, J.N. Weinstein, B. Kaminska, J. Huelsken, L. Omberg, O. Gevaert, A. Colaprico, P. Czerwinska, S. Mazurek, L. Mishra, H. Heyn, A. Krasnitz, A.K. Godwin, A.J. Lazar, N. Cancer Genome Atlas Research, J.M. Stuart, K.A. Hoadley, P.W. Laird, H. Noushmehr, M. Wiznerowicz, Machine learning identifies stemness features associated with oncogenic dedifferentiation, Cell 173 (2) (2018) 338–354 e15.
[10] N. Skrypek, S. Goossens, E. De Smedt, N. Vandamme, G. Berx, Epithelial-to-Mesenchymal transition: epigenetic reprogramming driving cellular plasticity, Trends Genet. 33 (12) (2017) 943–959.
[11] K.T. Yeung, J. Yang, Epithelial-mesenchymal transition in tumor metastasis, Mol. Oncol. 11 (1) (2017) 28–39.
[12] S. Lamouille, J. Xu, R. Derynck, Molecular mechanisms of epithelial-mesenchymal transition, Nat. Rev. Mol. Cell Biol. 15 (3) (2014) 178–196.
[13] P. Zhou, B. Li, F. Liu, M. Zhang, Q. Wang, Y. Liu, Y. Yao, D. Li, The epithelial to mesenchymal transition (EMT) and cancer stem cells: implication for treatment resistance in pancreatic cancer, Mol. Cancer 16 (1) (2017) 52.
[14] G. Pan, Y. Liu, L. Shang, F. Zhou, S. Yang, EMT-associated microRNAs and their roles in cancer stemness and drug resistance, Cancer Commun. 41 (3) (2021) 199–217.
[15] M. Shackleton, E. Quintana, E.R. Fearon, S.J. Morrison, Heterogeneity in cancer: cancer stem cells versus clonal evolution, Cell 138 (5) (2009) 822–829.
[16] M.H. Frank, B.J. Wilson, J.S. Gold, N.Y. Frank, Clinical implications of colorectal cancer stem cells in the age of single-cell omics and targeted therapies, Gastroenterology 160 (6) (2021) 1947–1960.
[17] M. Idorn, P. Thor Straten, Exercise and cancer: from "healthy" to "therapeutic"? Cancer Immunol. Immunother. 66 (5) (2017) 667–671.
[18] Z.W. Luo, Y.Y. Sun, W. Xia, J.Y. Xu, D.J. Xie, C.M. Jiao, J.Z. Dong, H. Chen, R.W. Wan, S.Y. Chen, J. Mei, W.J. Mao, Physical exercise reverses immuno-cold tumor microenvironment via inhibiting SQLE in non-small cell lung cancer, Mil. Med. Res. 10 (1) (2023) 39.
[19] Z. Luo, R. Wan, S. Liu, X. Feng, Z. Peng, Q. Wang, S. Chen, X. Shang, Mechanisms of exercise in the treatment of lung cancer - a mini-review, Front. Immunol. 14 (2023) 1244764.
[20] C.M. Friedenreich, H.K. Neilson, M.S. Farris, K.S. Courneya, Physical activity and cancer outcomes: a precision medicine approach, Clin. Cancer Res. 22 (19) (2016) 4766–4775.
[21] G.J. Koelwyn, D.F. Quail, X. Zhang, R.M. White, L.W. Jones, Exercise-dependent regulation of the tumour microenvironment, Nat. Rev. Cancer 17 (10) (2017) 620–632.

[22] Z. Luo, Z. He, H. Qin, Y. Chen, B. Qi, J. Lin, Y. Sun, J. Sun, X. Su, Z. Long, S. Chen, Exercise-induced IL-15 acted as a positive prognostic implication and tumor-suppressed role in pan-cancer, Front. Pharmacol. 13 (2022) 1053137.
[23] X. Gu, L. Cai, Z. Luo, L. Shi, Z. Peng, Y. Sun, J. Chen, Identification and validation of a muscle failure index to predict prognosis and immunotherapy in lung adenocarcinoma through integrated analysis of bulk and single-cell RNA sequencing data, Front. Immunol. 13 (2022) 1057088.
[24] P.D. Neufer, M.M. Bamman, D.M. Muoio, C. Bouchard, D.M. Cooper, B.H. Goodpaster, F.W. Booth, W.M. Kohrt, R.E. Gerszten, M.P. Mattson, R.T. Hepple, W. E. Kraus, M.B. Reid, S.C. Bodine, J.M. Jakicic, J.L. Fleg, J.P. Williams, L. Joseph, M. Evans, P. Maruvada, M. Rodgers, M. Roary, A.T. Boyce, J.K. Drugan, J. I. Koenig, R.H. Ingraham, D. Krotoski, M. Garcia-Cazarin, J.A. McGowan, M.R. Laughlin, Understanding the cellular and molecular mechanisms of physical activity-induced health benefits, Cell Metabol. 22 (1) (2015) 4–11.
[25] J.M. Peake, J.F. Markworth, K. Nosaka, T. Raastad, G.D. Wadley, V.G. Coffey, Modulating exercise-induced hormesis: does less equal more? J. Appl. Physiol. 119 (3) (2015) 172–189.
[26] J.S. Kim, D.A. Galvao, R.U. Newton, E. Gray, D.R. Taaffe, Exercise-induced myokines and their effect on prostate cancer, Nat. Rev. Urol. 18 (9) (2021) 519–542.
[27] H. Rundqvist, P. Velica, L. Barbieri, P.A. Gameiro, D. Bargiela, M. Gojkovic, S. Mijwel, S.M. Reitzner, D. Wulliman, E. Ahlstedt, J. Ule, A. Ostman, R.S. Johnson, Cytotoxic T-cells mediate exercise-induced reductions in tumor growth, Elife 9 (2020).
[28] M. Esteves, M.P. Monteiro, J.A. Duarte, Role of regular physical exercise in tumor vasculature: favorable modulator of tumor Milieu, Int. J. Sports Med. 42 (5) (2021) 389–406.
[29] L. Pedersen, M. Idorn, G.H. Olofsson, B. Lauenborg, I. Nookaew, R.H. Hansen, H.H. Johannesen, J.C. Becker, K.S. Pedersen, C. Dethlefsen, J. Nielsen, J. Gehl, B. K. Pedersen, P. Thor Straten, P. Hojman, Voluntary running suppresses tumor growth through epinephrine- and IL-6-dependent NK cell mobilization and redistribution, Cell Metabol. 23 (3) (2016) 554–562.
[30] J.S. Kim, R.L. Wilson, D.R. Taaffe, D.A. Galvao, E. Gray, R.U. Newton, Myokine expression and tumor-suppressive effect of serum after 12 wk of exercise in prostate cancer patients on ADT, Med. Sci. Sports Exerc. 54 (2) (2022) 197–205.
[31] E. Kurz, C.A. Hirsch, T. Dalton, S.A. Shadaloey, A. Khodadadi-Jamayran, G. Miller, S. Pareek, H. Rajaei, C. Mohindroo, S. Baydogan, A. Ngo-Huang, N. Parker, M.H.G. Katz, M. Petzel, E. Vucic, F. McAllister, K. Schadler, R. Winograd, D. Bar-Sagi, Exercise-induced engagement of the IL-15/IL-15Ralpha axis promotes anti-tumor immunity in pancreatic cancer, Cancer Cell (2022).
[32] M.M. Robinson, S. Dasari, A.R. Konopka, M.L. Johnson, S. Manjunatha, R.R. Esponda, R.E. Carter, I.R. Lanza, K.S. Nair, Enhanced protein translation underlies improved metabolic and physical adaptations to different exercise training modes in young and old humans, Cell Metabol. 25 (3) (2017) 581–592.
[33] M.E. Ritchie, B. Phipson, D. Wu, Y. Hu, C.W. Law, W. Shi, G.K. Smyth, Limma powers differential expression analyses for RNA-sequencing and microarray studies, Nucleic Acids Res. 43 (7) (2015) e47.
[34] Y. Chen, Y. Sun, Y. Xu, W.W. Lin, Z. Luo, Z. Han, S. Liu, B. Qi, C. Sun, K. Go, X.R. Kang, J. Chen, Single-cell integration analysis of heterotopic ossification and fibrocartilage developmental lineage: endoplasmic reticulum stress effector Xbp1 transcriptionally regulates the Notch signaling pathway to mediate fibrocartilage differentiation, Oxid. Med. Cell. Longev. 2021 (2021) 7663366.
[35] W. Lin, Y. Wang, Y. Chen, Q. Wang, Z. Gu, Y. Zhu, Role of calcium signaling pathway-related gene regulatory networks in ischemic stroke based on multiple WGCNA and single-cell analysis, Oxid. Med. Cell. Longev. 2021 (2021) 8060477.
[36] M.L. Suva, I. Tirosh, Single-cell RNA sequencing in cancer: lessons learned and emerging challenges, Mol. Cell 75 (1) (2019) 7–12.
[37] J.Y. Wu, J. Qin, L. Li, K.D. Zhang, Y.S. Chen, Y. Li, T. Jin, J.M. Xu, Roles of the immune/methylation/autophagy landscape on single-cell genotypes and stroke risk in breast cancer microenvironment, Oxid. Med. Cell. Longev. 2021 (2021) 5633514.
[38] Y. Chen, Y. Sun, Z. Luo, X. Chen, Y. Wang, B. Qi, J. Lin, W.W. Lin, C. Sun, Y. Zhou, J. Huang, Y. Xu, J. Chen, S. Chen, Exercise modifies the transcriptional regulatory features of monocytes in Alzheimer's patients: a multi-omics integration analysis based on single cell technology, Front. Aging Neurosci. 14 (2022) 881488.
[39] E. Becht, L. McInnes, J. Healy, C.A. Dutertre, I.W.H. Kwok, L.G. Ng, F. Ginhoux, E.W. Newell, Dimensionality reduction for visualizing single-cell data using UMAP, Nat. Biotechnol. 37 (2019) 38–44.
[40] N. Pezzotti, B.P.F. Lelieveldt, L. Van Der Maaten, T. Hollt, E. Eisemann, A. Vilanova, Approximated and user steerable tSNE for progressive visual analytics, IEEE Trans. Vis. Comput. Graph. 23 (7) (2017) 1739–1752.
[41] D. Aran, A.P. Looney, L. Liu, E. Wu, V. Fong, A. Hsu, S. Chak, R.P. Naikawadi, P.J. Wolters, A.R. Abate, A.J. Butte, M. Bhattacharya, Reference-based analysis of lung single-cell sequencing reveals a transitional profibrotic macrophage, Nat. Immunol. 20 (2) (2019) 163–172.
[42] M.I. Love, W. Huber, S. Anders, Moderated estimation of fold change and dispersion for RNA-seq data with DESeq2, Genome Biol. 15 (12) (2014) 550.
[43] Z. Zhang, Z.X. Wang, Y.X. Chen, H.X. Wu, L. Yin, Q. Zhao, H.Y. Luo, Z.L. Zeng, M.Z. Qiu, R.H. Xu, Integrated analysis of single-cell and bulk RNA sequencing data reveals a pan-cancer stemness signature predicting immunotherapy response, Genome Med. 14 (1) (2022) 45.
[44] M. Ghandi, F.W. Huang, J. Jane-Valbuena, G.V. Kryukov, C.C. Lo, E.R. McDonald 3rd, J. Barretina, E.T. Gelfand, C.M. Bielski, H. Li, K. Hu, A.Y. Andreev-Drakhlin, J. Kim, J.M. Hess, B.J. Haas, F. Aguet, B.A. Weir, M.V. Rothberg, B.R. Paolella, M.S. Lawrence, R. Akbani, Y. Lu, H.L. Tiv, P.C. Gokhale, A. de Weck, A. A. Mansour, C. Oh, J. Shih, K. Hadi, Y. Rosen, J. Bistline, K. Venkatesan, A. Reddy, D. Sonkin, M. Liu, J. Lehar, J.M. Korn, D.A. Porter, M.D. Jones, J. Golji, G. Caponigro, J.E. Taylor, C.M. Dunning, A.L. Creech, A.C. Warren, J.M. McFarland, M. Zamanighomi, A. Kauffmann, N. Stransky, M. Imielinski, Y.E. Maruvka, A.D. Cherniack, A. Tsherniak, F. Vazquez, J.D. Jaffe, A.A. Lane, D.M. Weinstock, C.M. Johannessen, M.P. Morrissey, F. Stegmeier, R. Schlegel, W.C. Hahn, G. Getz, G.B. Mills, J.S. Boehm, T.R. Golub, L.A. Garraway, W.R. Sellers, Next-generation characterization of the cancer cell line encyclopedia, Nature 569 (7757) (2019) 503–508.
[45] S. Hanzelmann, R. Castelo, J. Guinney, GSVA: gene set variation analysis for microarray and RNA-seq data, BMC Bioinf. 14 (2013) 7.
[46] G. Bindea, B. Mlecnik, M. Tosolini, A. Kirilovsky, M. Waldner, A.C. Obenauf, H. Angell, T. Fredriksen, L. Lafontaine, A. Berger, P. Bruneval, W.H. Fridman, C. Becker, F. Pages, M.R. Speicher, Z. Trajanoski, J. Galon, Spatiotemporal dynamics of intratumoral immune cells reveal the immune landscape in human cancer, Immunity 39 (4) (2013) 782–795.
[47] V. Thorsson, D.L. Gibbs, S.D. Brown, D. Wolf, D.S. Bortone, T.H. Ou Yang, E. Porta-Pardo, G.F. Gao, C.L. Plaisier, J.A. Eddy, E. Ziv, A.C. Culhane, E.O. Paull, I.K. A. Sivakumar, A.J. Gentles, R. Malhotra, F. Farshidfar, A. Colaprico, J.S. Parker, L.E. Mose, N.S. Vo, J. Liu, Y. Liu, J. Rader, V. Dhankani, S.M. Reynolds, R. Bowlby, A. Califano, A.D. Cherniack, D. Anastassiou, D. Bedognetti, Y. Mokrab, A.M. Newman, A. Rao, K. Chen, A. Krasnitz, H. Hu, T.M. Malta, H. Noushmehr, C.S. Pedamallu, S. Bullman, A.I. Ojesina, A. Lamb, W. Zhou, H. Shen, T.K. Choueiri, J.N. Weinstein, J. Guinney, J. Saltz, R.A. Holt, C.S. Rabkin, N. Cancer Genome Atlas Research, A.J. Lazar, J.S. Serody, E.G. Demicco, M.L. Disis, B.G. Vincent, I. Shmulevich, The immune landscape of cancer, Immunity 48 (4) (2018) 812–830 e14.
[48] J. Hu, A. Yu, B. Othmane, D. Qiu, H. Li, C. Li, P. Liu, W. Ren, M. Chen, G. Gong, X. Guo, H. Zhang, J. Chen, X. Zu, Siglec15 shapes a non-inflamed tumor microenvironment and predicts the molecular subtype in bladder cancer, Theranostics 11 (7) (2021) 3089–3108.
[49] J. Mei, Y. Cai, R. Xu, Y. Zhu, X. Zhao, Y. Zhang, W. Mao, J. Xu, Y. Yin, Protocol to identify novel immunotherapy biomarkers based on transcriptomic data in human cancers, STAR Protocols 4 (2) (2023) 102258.
[50] K. Yoshihara, M. Shahmoradgoli, E. Martinez, R. Vegesna, H. Kim, W. Torres-Garcia, V. Trevino, H. Shen, P.W. Laird, D.A. Levine, S.L. Carter, G. Getz, K. Stemke-Hale, G.B. Mills, R.G. Verhaak, Inferring tumour purity and stromal and immune cell admixture from expression data, Nat. Commun. 4 (2013) 2612.
[51] G. Yu, L.G. Wang, Y. Han, Q.Y. He, clusterProfiler: an R package for comparing biological themes among gene clusters, OMICS 16 (5) (2012) 284–287.
[52] A. Subramanian, P. Tamayo, V.K. Mootha, S. Mukherjee, B.L. Ebert, M.A. Gillette, A. Paulovich, S.L. Pomeroy, T.R. Golub, E.S. Lander, J.P. Mesirov, Gene set enrichment analysis: a knowledge-based approach for interpreting genome-wide expression profiles, Proc. Natl. Acad. Sci. U. S. A. 102 (43) (2005) 15545–15550.
[53] Z. Luo, Y. Sun, B. Qi, J. Lin, Y. Chen, Y. Xu, J. Chen, Human bone marrow mesenchymal stem cell-derived extracellular vesicles inhibit shoulder stiffness via let-7a/Tgfbr1 axis, Bioact. Mater. 17 (2022) 344–359.
[54] J. Mei, Y. Liu, X. Yu, L. Hao, T. Ma, Q. Zhan, Y. Zhang, Y. Zhu, YWHAZ interacts with DAAM1 to promote cell migration in breast cancer, Cell Death Dis. 7 (1) (2021) 221.

[55] S. Li, J. Yu, A. Huber, I. Kryczek, Z. Wang, L. Jiang, X. Li, W. Du, G. Li, S. Wei, L. Vatan, W. Szeliga, A.M. Chinnaiyan, M.D. Green, M. Cieslik, W. Zou, Metabolism drives macrophage heterogeneity in the tumor microenvironment, Cell Rep. 39 (1) (2022) 110609.
[56] D. Aran, M. Sirota, A.J. Butte, Systematic pan-cancer analysis of tumour purity, Nat. Commun. 6 (2015) 8971.
[57] M. Ju, J. Bi, Q. Wei, L. Jiang, Q. Guan, M. Zhang, X. Song, T. Chen, J. Fan, X. Li, M. Wei, L. Zhao, Pan-cancer analysis of NLRP3 inflammasome with potential implications in prognosis and immunotherapy in human cancer, Briefings Bioinf. 22 (4) (2021).
[58] A. Bagaev, N. Kotlov, K. Nomie, V. Svekolkin, A. Gafurov, O. Isaeva, N. Osokin, I. Kozlov, F. Frenkel, O. Gancharova, N. Almog, M. Tsiper, R. Ataullakhanov, N. Fowler, Conserved pan-cancer microenvironment subtypes predict response to immunotherapy, Cancer Cell 39 (6) (2021) 845–865 e7.
[59] N. Li, Y. Li, P. Zheng, X. Zhan, Cancer stemness-based prognostic immune-related gene signatures in lung adenocarcinoma and lung squamous cell carcinoma, Front. Endocrinol. 12 (2021) 755805.
[60] G. Bi, D. Zhu, Y. Bian, Y. Huang, C. Zhan, Y. Yang, Q. Wang, Knockdown of GTF2E2 inhibits the growth and progression of lung adenocarcinoma via RPS4X in vitro and in vivo, Cancer Cell Int. 21 (1) (2021) 181.
[61] C. Zhou, C. Liu, W. Liu, W. Chen, Y. Yin, C.W. Li, J.L. Hsu, J. Sun, Q. Zhou, H. Li, B. Hu, P. Fu, M. Atyah, Q. Ma, Y. Xu, Q. Dong, M.C. Hung, N. Ren, SLFN11 inhibits hepatocellular carcinoma tumorigenesis and metastasis by targeting RPS4X via mTOR pathway, Theranostics 10 (10) (2020) 4627–4643.
[62] I. Vitale, G. Manic, L.M. Coussens, G. Kroemer, L. Galluzzi, Macrophages and metabolism in the tumor microenvironment, Cell Metabol. 30 (1) (2019) 36–50.
[63] J.E. Bader, K. Voss, J.C. Rathmell, Targeting metabolism to improve the tumor microenvironment for cancer immunotherapy, Mol. Cell 78 (6) (2020) 1019–1033.
[64] Y. Xiao, D. Yu, Tumor microenvironment as a therapeutic target in cancer, Pharmacol. Ther. 221 (2021) 107753.
[65] O. Meurette, P. Mehlen, Notch signaling in the tumor microenvironment, Cancer Cell 34 (4) (2018) 536–548.
[66] T. Wu, Y. Dai, Tumor microenvironment and therapeutic response, Cancer Lett. 387 (2017) 61–68.
[67] Y. Chen, K.M. McAndrews, R. Kalluri, Clinical and therapeutic relevance of cancer-associated fibroblasts, Nat. Rev. Clin. Oncol. 18 (12) (2021) 792–804.
[68] J.D. Lathia, H. Liu, Overview of cancer stem cells and stemness for community oncologists, Targeted Oncol. 12 (4) (2017) 387–399.
[69] L. Walcher, A.K. Kistenmacher, H. Suo, R. Kitte, S. Dluczek, A. Strauss, A.R. Blaudszun, T. Yevsa, S. Fricke, U. Kossatz-Boehlert, Cancer stem cells-origins and biomarkers: perspectives for targeted personalized therapies, Front. Immunol. 11 (2020) 1280.
[70] X. Jiao, X. Qian, L. Wu, B. Li, Y. Wang, X. Kong, L. Xiong, microRNA: the impact on cancer stemness and therapeutic resistance, Cells 9 (1) (2019).
[71] S. Prasad, S. Ramachandran, N. Gupta, I. Kaushik, S.K. Srivastava, Cancer cells stemness: a doorstep to targeted therapy, Biochim. Biophys. Acta, Mol. Basis Dis. 1866 (4) (2020) 165424.
[72] B. Song, D.K. Kim, J. Shin, S.H. Bae, H.Y. Kim, B. Won, J.K. Kim, H.D. Youn, S.T. Kim, S.W. Kang, H. Jang, OCT4 directly regulates stemness and extracellular matrix-related genes in human germ cell tumours, Biochem. Biophys. Res. Commun. 503 (3) (2018) 1980–1986.
[73] J. Lu, G. Song, Q. Tang, J. Yin, C. Zou, Z. Zhao, X. Xie, H. Xu, G. Huang, J. Wang, D.F. Lee, R. Khokha, H. Yang, J. Shen, MiR-26a inhibits stem cell-like phenotype and tumor growth of osteosarcoma by targeting Jagged1, Oncogene 36 (2) (2017) 231–241.
[74] A.P. Deshmukh, S.V. Vasaikar, K. Tomczak, S. Tripathi, P. den Hollander, E. Arslan, P. Chakraborty, R. Soundararajan, M.K. Jolly, K. Rai, H. Levine, S.A. Mani, Identification of EMT signaling cross-talk and gene regulatory networks by single-cell RNA sequencing, Proc. Natl. Acad. Sci. U. S. A. 118 (19) (2021).
[75] H. Schinke, E. Shi, Z. Lin, T. Quadt, G. Kranz, J. Zhou, H. Wang, J. Hess, S. Heuer, C. Belka, H. Zitzelsberger, U. Schumacher, S. Genduso, K. Riecken, Y. Gao, Z. Wu, C.A. Reichel, C. Walz, M. Canis, K. Unger, P. Baumeister, M. Pan, O. Gires, A transcriptomic map of EGFR-induced epithelial-to-mesenchymal transition identifies prognostic and therapeutic targets for head and neck cancer, Mol. Cancer 21 (1) (2022) 178.
[76] V. Mittal, Epithelial mesenchymal transition in tumor metastasis, Annu. Rev. Pathol. 13 (2018) 395–412.
[77] A. Dongre, R.A. Weinberg, New insights into the mechanisms of epithelial-mesenchymal transition and implications for cancer, Nat. Rev. Mol. Cell Biol. 20 (2) (2019) 69–84.
[78] E.M. Fisher, P. Beer-Romero, L.G. Brown, A. Ridley, J.A. McNeil, J.B. Lawrence, H.F. Willard, F.R. Bieber, D.C. Page, Homologous ribosomal protein genes on the human X and Y chromosomes: escape from X inactivation and possible implications for Turner syndrome, Cell 63 (6) (1990) 1205–1218.
[79] S.P. Tsofack, L. Meunier, L. Sanchez, J. Madore, D. Provencher, A.M. Mes-Masson, M. Lebel, Low expression of the X-linked ribosomal protein S4 in human serous epithelial ovarian cancer is associated with a poor prognosis, BMC Cancer 13 (2013) 303.
[80] E.R. Paquet, H. Hovington, H. Brisson, C. Lacombe, H. Larue, B. Tetu, L. Lacombe, Y. Fradet, M. Lebel, Low level of the X-linked ribosomal protein S4 in human urothelial carcinomas is associated with a poor prognosis, Biomarkers Med. 9 (3) (2015) 187–197.
[81] J. Kuang, Q.Y. Li, F. Fan, N.J. Shen, Y.J. Zhan, Z.H. Tang, W.L. Yu, Overexpression of the X-linked ribosomal protein S4 predicts poor prognosis in patients with intrahepatic cholangiocarcinoma, Oncol. Lett. 14 (1) (2017) 41–46.
[82] G. Schneider, M. Schmidt-Supprian, R. Rad, D. Saur, Tissue-specific tumorigenesis: context matters, Nat. Rev. Cancer 17 (4) (2017) 239–253.
[83] Z. Luo, R. Wan, S. Liu, X. Feng, Z. Peng, Q. Wang, S. Chen, X. Shang, Mechanisms of exercise in the treatment of lung cancer – a mini-review, Front. Immunol. 14 (2023).
[84] S.C. Moore, I.M. Lee, E. Weiderpass, P.T. Campbell, J.N. Sampson, C.M. Kitahara, S.K. Keadle, H. Arem, A. Berrington de Gonzalez, P. Hartge, H.O. Adami, C. K. Blair, K.B. Borch, E. Boyd, D.P. Check, A. Fournier, N.D. Freedman, M. Gunter, M. Johannson, K.T. Khaw, M.S. Linet, N. Orsini, Y. Park, E. Riboli, K. Robien, C. Schairer, H. Sesso, M. Spriggs, R. Van Dusen, A. Wolk, C.E. Matthews, A.V. Patel, Association of leisure-time physical activity with risk of 26 types of cancer in 1.44 million adults, JAMA Intern. Med. 176 (6) (2016) 816–825.
[85] L. Pedersen, J.F. Christensen, P. Hojman, Effects of exercise on tumor physiology and metabolism, Cancer J. 21 (2) (2015) 111–116.
[86] D. Kostrzewa-Nowak, J. Kubaszewska, A. Nowakowska, R. Nowak, Effect of aerobic and anaerobic exercise on the complement system of proteins in healthy young males, J. Clin. Med. 9 (8) (2020).
[87] G. Holmen Olofsson, A.W.P. Jensen, M. Idorn, P. Thor Straten, Exercise oncology and immuno-oncology; A (future) dynamic duo, Int. J. Mol. Sci. 21 (11) (2020).
[88] A. Pahl, A. Wehrle, S. Kneis, A. Gollhofer, H. Bertz, Feasibility of whole body vibration during intensive chemotherapy in patients with hematological malignancies - a randomized controlled pilot study, BMC Cancer 18 (1) (2018) 920.
[89] J.F. Christensen, C. Simonsen, P. Hojman, Exercise training in cancer control and treatment, Compr. Physiol. 9 (1) (2018) 165–205.
[90] B.M. Gabriel, D.L. Hamilton, A.M. Tremblay, H. Wackerhage, The Hippo signal transduction network for exercise physiologists, J. Appl. Physiol. 120 (10) (2016) 1105–1117.